ground water

Mass Discharge in a Tracer Plume: Evaluation of the Theissen Polygon Method

by Douglas M. Mackay[1], Murray D. Einarson[2], Phil M. Kaiser[3], Mamie Nozawa-Inoue[3], Sham Goyal[3], Irina Chakraborty[3], Ehsan Rasa[3], and Kate M. Scow[3]

Abstract

A tracer plume was created within a thin aquifer by injection for 299 d of two adjacent "sub-plumes" to represent one type of plume heterogeneity encountered in practice. The plume was monitored by snapshot sampling of transects of fully screened wells. The mass injection rate and total mass injected were known. Using all wells in each transect (0.77 m well spacing, 1.4 points/m^2 sampling density), the Theissen Polygon Method (TPM) yielded apparently accurate mass discharge (M_d) estimates at three transects for 12 snapshots. When applied to hypothetical sparser transects using subsets of the wells with average spacing and sampling density from 1.55 to 5.39 m and 0.70 to 0.20 points/m^2, respectively, the TPM accuracy depended on well spacing and location of the wells in the hypothesized transect with respect to the sub-plumes. Potential error was relatively low when the well spacing was less than the widths of the sub-plumes (>0.35 points/m^2). Potential error increased for well spacing similar to or greater than the sub-plume widths, or when less than 1% of the plume area was sampled. For low density sampling of laterally heterogeneous plumes, small changes in groundwater flow direction can lead to wide fluctuations in M_d estimates by the TPM. However, sampling conducted when flow is known or likely to be in a preferred direction can potentially allow more useful comparisons of M_d over multiyear time frames, such as required for performance evaluation of natural attenuation or engineered remediation systems.

Introduction

Contaminant mass discharge (M_d) is the rate of migration of dissolved contaminant mass (e.g., g/d) past a plane of reference orthogonal to groundwater flow. M_d measurements can provide a meaningful way to express relative source zone strength, potential downgradient impact, and efficiency of in situ treatment (Feenstra et al. 1996; Einarson and Mackay 2001; Rao et al. 2002; Pope et al. 2004; Clements et al. 2008; ITRC 2010; Newell et al. 2011). There have been several evaluations of various methods for estimating contaminant M_d; see review by Béland-Pelletier et al. (2011). The most commonly compared methods are based on: (1) sampling of transects of single or multilevel wells, generally interpreted using the Theissen Polygon Method (TPM), (2) integral pump tests conducted in wells across the plume, and (3) passive flux meters, that is, devices installed in wells across the plume which allow estimation of the groundwater flowing through the well and the amount of mass conveyed by the groundwater. Most of the studies have been based on monitoring of plumes emanating from accidental releases ("real" plumes) in various hydrogeological settings (Béland-Pelletier et al. 2011; Cai et al. 2011; Dietze and Dietrich 2011). While of enormous value, particularly in comparing different M_d estimation methods applied to the plumes, these studies are hampered by lack of knowledge of the true value of mass discharge at the time and location of sampling. Other efforts have

[1]Corresponding author: Department of Land, Air & Water Resources, University of California, One Shields Avenue, Davis, CA 95616; 1-650-324-2809; fax: 1-650-618-1571; dmmackay@ucdavis.edu

[2]AMEC Geomatrix Consultants, Inc., Oakland, CA 94612.

[3]University of California, Davis, CA 95616.

Received July 2011, accepted January 2012.

doi: 10.1111/j.1745-6584.2012.00912.x

used computer simulations to create synthetic data subsets which are then analyzed by one or more of the M_d estimation methods and the results compared to the "true" value of mass discharge defined by the model (Kübert and Finkel 2006; Li et al. 2007). These studies have provided complementary insights, but sufficiently detailed field data have not been available to date to confirm or refine an understanding of the critical issues in M_d estimation.

Li et al. (2007) stated that "In the field, it is impossible to measure the "true value" of the mass discharge . . . ," pointing out that "the true value should be known to evaluate . . . mass discharge uncertainty." To overcome this dilemma, which is inescapable for "real" plumes, we created a plume with known mass injection rate and total mass injected and then tested several M_d estimation methods using transects of wells and typical sampling methods. An overview of the complete research program is provided elsewhere (Malcolm Pirnie 2009). This paper describes the site, the experimental setup, and the results from one of the methods evaluated, that is, that based on sampling of wells in transects ("snapshot" sampling) and interpretation by the TPM. Thus, hereafter we restrict discussion to the snapshot/TPM method.

On the basis of numerical sampling of a simulated contaminant plume, Kübert and Finkel (2006) concluded for snapshot sampling that the estimation error was dependent on the sampling resolution and the aquifer heterogeneity (which controlled plume heterogeneity in their simulations since they assumed a uniform planar source). Research over the last decade has shown that chlorinated solvents and other contaminated plumes are often composed of a number of "sub-plumes" migrating alongside one another (Chapman et al. 1997; Guilbeault et al. 2005), in part arising from heterogeneity of the source itself. Thus, the spatial complexity of plumes at transects may typically arise from both the source heterogeneity as well as aquifer heterogeneity along the flowpaths from source to transect. Li et al. (2007) applied a geostatistical approach to address plume and aquifer heterogeneity during estimation of mass discharge using transects of multilevel wells. Cai et al. (2011) used a different geostatistical approach applied to field data, involving high-resolution interpolation to generate a detailed synthetic dataset from which mass discharge and its uncertainty were estimated. These insights were expanded by Béland-Pelletier et al. (2011) and Dietze and Dietrich (2011), who emphasized that uncertainty in M_d estimates by the TPM are directly related to the sampling density across the transect (sampling points per m^2) while accuracy was probably most strongly influenced by errors in understanding of groundwater discharge at the sampled locations.

In this paper, we evaluate the accuracy and potential error of M_d estimation based on snapshot transect sampling of a moderately heterogeneous, experimentally created tracer plume. This allows insights not possible from monitoring of real contaminant plumes (i.e., with unknown mass discharge and total mass), confirms conclusions of prior studies with synthetic datasets, and allows additional insights into sources of uncertainty in mass discharge estimates.

Experimental Site

Vandenberg Air Force Base (VAFB) is located near Santa Barbara, California. At VAFB Site 60 (Figure 1) a gasoline leak occurred at a fuel service station in 1994. In 1995, the tanks and piping were excavated and the excavation backfilled. The regional setting, site hydrogeology, and fate of petroleum and fuel oxygenate contamination have been described previously (Mackay et al. 2006). Petroleum hydrocarbons did not migrate far from the source and had naturally attenuated prior to the start of this work. On the basis of monitoring by UC Davis, the approximate areal extent of the oxygenate plume at the start of this study, containing methyl *tert*-butyl ether (MTBE) and *tert*-butyl alcohol (TBA), is shown in Figure 1.

VAFB Site 60 is underlain by alluvial sands, silts, and clays. A vertical schematic of the subsurface is presented in Figure 2 (Mackay et al. 2006). The primary pathway for migration of contaminants in groundwater is the S3 aquifer, which is approximately 0.9 m thick. The total porosity of the S3 was previously estimated as 0.34 based on core samples near the EAA transect (Mackay et al. 2006, supporting information). The S3 aquifer is present throughout the experimental zone and confined above and below by low permeability layers that are laterally continuous throughout and beyond the experimental

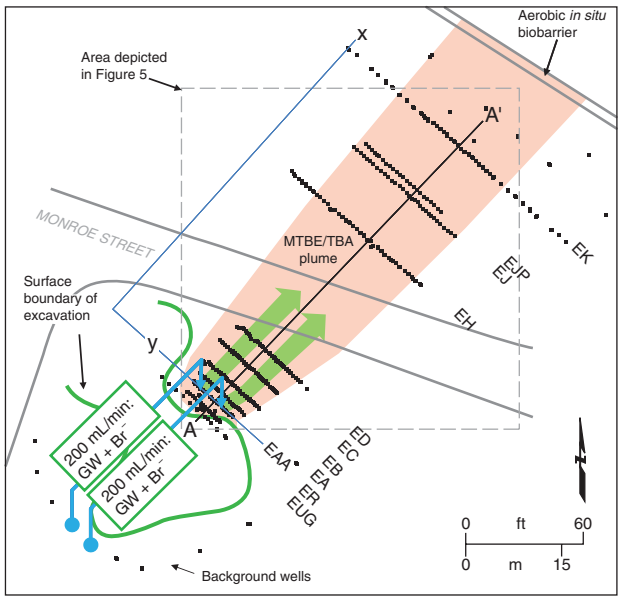

Figure 1. Map of experimental site. Dashed box encloses area depicted in frames of Figure 5. Details include boundary of excavation of original 1994 fuel spill and setup for the bromide tracer test. Supply wells are noted by blue circles, while the general injection locations are indicated by blue arrows. The expected bromide "sub-plumes" are shown by the broad green arrows. Black dots indicate monitoring wells. AA′ denotes the location of the vertical cross section in Figure 2. The *x* and *y* axes indicate the coordinate system used to define distances used in text and figures.

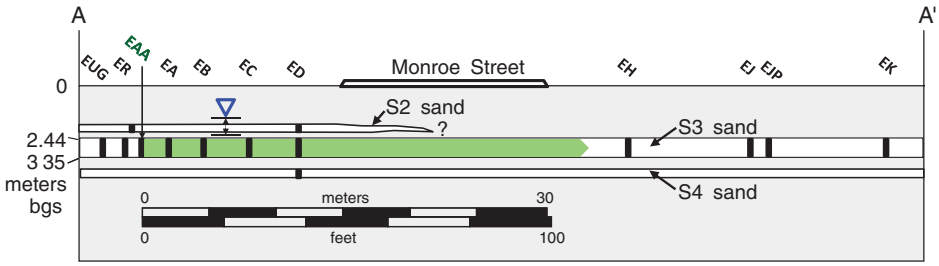

Figure 2. Vertical schematic illustrating the thin sandy aquifer (S3) and the approximate locations of the transects of wells. The injection of bromide-spiked groundwater into the S3 occurred in the EAA transect, indicated by the vertical arrow. Vertical exaggeration is approximately 1.25:1.

zone. Also shown in Figure 2 are the locations of the transects of wells, and the location of the experimental injection of bromide for this research. In field studies before this work, groundwater velocity had been estimated in various locations at the site to vary seasonally from 0.50 to 0.75 m/d, with higher velocities previously believed to be short-term transients during the brief winter rainy season.

Experimental Methods

A conceptual overview of the experiment is provided in Figures 1 and 2. Two adjacent "sub-plumes" of bromide tracer were created by injecting groundwater spiked with tracer into two sets of three wells each for approximately 10 months. Snapshot monitoring of the various transects was conducted from before the bromide injection to several months afterward.

Construction of the wells was described before (Mackay et al. 2006). The 1.3 cm wells were screened across the entire thickness of the S3 sand. Average distances between the wells in the ED, EH, and EJ transects were 0.52, 0.77, and 0.77 m, respectively. Piezometric head was measured by standard methods using approximately 50 wells on 12 occasions before, during, and after the bromide injection.

Injection wells (Figures 1 and 3) created two bromide sub-plumes side by side to represent plume heterogeneity arising initially from source heterogeneity. Groundwater was extracted from two background wells, spiked with a small flow of concentrated bromide solution, and then re-injected into six wells: EAA 4, 5, 6 created the western sub-plume (Lane A) and EAA 11, 12, 13 created the eastern sub-plume (Lane B). Peristaltic pumps controlled groundwater extraction and total flow rate. Bromide-spiked groundwater was injected at an average total rate of 200 mL/min into each lane. Concentrated bromide spike solutions were made by dissolving weighed masses of reagent grade potassium bromide into measured volumes of water. Spike solution was metered into the main water flow (Figure 3) using a high performance liquid chromatography (HPLC) pump. New spike solutions were added to the reservoir 43 times during 10 months of tracer injection. Injection rate and cumulative bromide mass injected were determined from volumes/concentrations of tracer spike solution used.

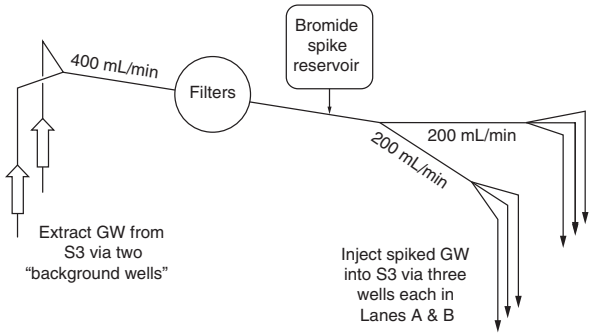

Figure 3. Schematic of the injection system. Two background wells were used to supply approximately 400 mL/min of groundwater, which were then spiked with a concentrated bromide solution, split into six approximately equal flows, and directed into six individual injection wells in the EAA transect: three to create the west sub-plume (Lane A) and three to create the east sub-plume (Lane B).

Groundwater samples were collected as described by Mackay et al. (2006); prior work had shown that purging 300 mL from the wells was sufficient to recover samples that represented the monitored interval. Duplicate bromide samples were collected in 8 mL LDPE bottles without preservative; also, though not discussed herein, duplicate VOC samples were collected in 22 mL glass vials. Bromide samples were stored at room temperature.

Samples were analyzed for bromide at UC Davis by HPLC with an electrical conductivity detector. The method is described in detail by Malcolm Pirnie (2009). Calibration checks were run each day of analyses. The method detection limit was 0.29 mg/L (practical quantification limit ~1.5 mg/L). The precision of 20 lab duplicate samples was 0.65% as a mean relative percent difference (RPD). Monitoring during the experiment indicated that natural background bromide levels varied slightly over time and space, with an average value of 3.1 mg/L. All raw analytical estimates of bromide concentrations were corrected by subtracting 3.1 mg/L before use in calculations. If the raw measured concentration was below the average background value, the corrected value was set to zero. Areal plots of corrected bromide concentration contours were produced with Surfer software (Golden, CO), as used for other solutes in prior research at this site (Mackay et al. 2006).

The bromide M_d through a transect was estimated using the TPM:

$$M_{d,j} = \sum_{k=1}^{n_w} C_{k,j} K_k i_k A_k \quad (1)$$

where $M_{d,j}$ is the mass discharge (g/d) at a given time j, $C_{k,j}$ is the concentration of the solute in samples (g/m^3) from monitoring well k at time j, K_k is the hydraulic conductivity of the aquifer (m/d) at the location of monitoring well k, i_k is the hydraulic gradient (−) at monitoring well k, A_k is the cross-sectional discharge area (m^2) of the aquifer assumed represented by monitoring well k, and n_w is the number of wells in the control plane. In this research, as discussed later, concentration is the only term that changes significantly over time, and K_k and i_k are assumed constant in space and time in the experimental area.

The cross-sectional area within the aquifer assumed to be represented by each well was estimated as the thickness of the aquifer times the width sampled, the latter equal to the sum of half the distances to the two nearest wells in opposite directions (except for end wells, for which the sampled width was assumed to be the distance to the nearest well). The aquifer thickness, measured during previous site investigations, was set at an average value of 0.9 m for these calculations.

EJP wells (Figure 1) were pumped intermittently at low rates during this experiment to evaluate another method of measuring M_d (see Malcolm Pirnie 2009). Intermittent pumping of groundwater from the EJP wells likely created a minor increase in the groundwater velocity flowing through the EJ transect, as discussed below. Timing and duration of pumping at the EJP transect are listed in Table 1.

Table 1
Type and Timing of Key Events

Category	Event	Start Date	Elapsed Days	End Date	Elapsed Days	Wells or Transects Involved	Result or Comment
Injection							
	Water + Bromide	July 11, 2005	0	May 6, 2006	299	EAA 4,5,6,11,12,13	—
	Water	May 6, 2006	299	August 24, 2006	409	EAA 4,5,6,11,12,13	—
Water levels						Transects used in gradient estimation	Gradient ± 95%CI
	WL #1	May 9, 2005	−63	May 9, 2005	−63	EC, ED, EH	0.0123 ± 0.0006
	WL #2	August 16, 2005	36	August 16, 2005	36	EC, ED, EH	0.0133 ± 0.0006
	WL #3	October 13, 2005	94	October 13, 2005	94	EC, ED, EH	0.0142 ± 0.0005
	WL #4	December 14, 2005	156	December 14, 2005	156	EH, EJ	0.0134 ± 0.0009
	WL #5	January 12, 2006	185	January 12, 2006	185	EC, ED, EH	Data unreliable
	WL #6	February 22, 2006	226	February 22, 2006	226	EC, ED, EH	0.0136 ± 0.0011
	WL #7	March 17, 2006	249	March 17, 2006	249	ED, EH	0.0136 ± 0.0010
	WL #8	April 20, 2006	283	April 20, 2006	283	ED, EH	0.0121 ± 0.0011
	WL #9	May 18, 2006	311	May 18, 2006	311	ED, EH	0.0135 ± 0.0006
	WL #10	July 11, 2006	365	July 11, 2006	365	EC, ED, EH, EJ	0.0122 ± 0.0006
	WL #11	August 29, 2006	414	August 29, 2006	414	EC, ED, EH	Data unreliable
	WL #12	November 13, 2006	490	November 13, 2006	490	ED, EH, EJ	0.0135 ± 0.0005
	WL #13	April 2, 2007	630	April 2, 2007	630	ED, EH, EJ	0.0132 ± 0.0003
Passive fluxmeter deployment in subsets of EJP wells							Impact on water level
	PFM #1 and #2	December 6, 2005	148	December 12, 2005	154	All 23 then 11 in EJP	Insertion/removal cause brief local head rise/drop, resp.
	PFM #3	April 21, 2006	284	April 24, 2006	287	19 in EJP	
Pumping of subsets of EJP wells ("Steady State Pumping" or SSP)						Wells pumped	Pumping rate/well (L/min)
	SSP #1	December 15, 2005	157	March 17, 2006	249	All 23 EJP	<0.06 L/min
	SSP #2	April 7, 2006	270	April 18, 2006	281	All 23 EJP	<0.06 L/min
	SSP #3	May 31, 2006	324	June 20, 2006	344	6 in EJP	<0.2 mL/min
Hydraulic testing (short-term pumping) of subsets of EJP wells						Wells pumped	Pumping rate/well (L/min)
	Pumping Tests	March 24, 2006	256	March 24, 2006	256	All 23 EJP	0.18–2.9 L/min
	Pumping Tests	March 27, 2006	259	March 27, 2006	259	All 23 EJP	0.08–1.53 L/min

Notes: Elapsed days refer to days after (or before, if negative) initiation of water and bromide injection.

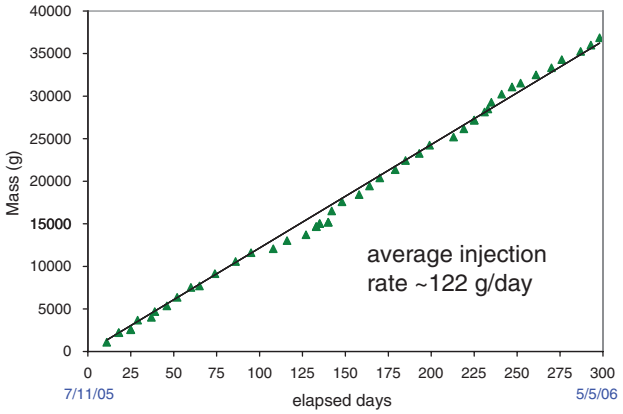

Figure 4. Bromide injection history (cumulative injected mass vs. time). The start and stop dates for injection are noted in blue. Linear regression (black line) yields average injection rate as shown.

Results and Discussion

Creation and Monitoring of the Bromide Plume

The controlled injection of bromide-spiked groundwater began on July 11, 2005, and continued for 299 d, ending May 6, 2006 (Table 1). The injection system operated continuously, with only short (1 to 2 h) interruptions for weekly maintenance. After bromide addition ended, injection of unspiked groundwater continued for 110 d.

Figure 4 depicts the cumulative mass of bromide injected vs. time. The rate of bromide injection averaged 122 g/d but varied somewhat throughout the period. Because bromide behaves as a conservative tracer, the mass injection rate is equal to the mass discharge in the aquifer immediately downgradient of the injection wells. The total mass of bromide injected was 36.86 kg. The uncertainty in the total injected mass is low, on the order of ±0.2 kg (<1%).

The spatial distribution of bromide was monitored in snapshots, each of which sampled all or a subset of the wells. Generally sampling of a specific transect was completed in a single day. A total of 7185 samples were collected and analyzed, resulting in removal of approximately 380 mL of water for each sampling at each location (purge plus duplicate bromide and VOC samples). Approximately 137 g (<0.4%) of the injected bromide was removed from the aquifer by the purging and sampling process.

Figure 5 displays bromide isoconcentration contour plots from four of the spatial snapshots. The top frames of Figure 5 depict the growth of the bromide sub-plumes, while the bottom frames depict the flushing of the bromide sub-plumes after bromide injection ended. The bromide plume had moderate spatial and temporal variability, confirmed in the contour plots from the other snapshots (not shown).

Figure 6 presents plots of the bromide concentration across the EH transect for all snapshots. Plots are similar for the other transects, confirming that the sub-plumes were well-defined by the sampling network. Figures 5 and 6 show that lateral dispersion was weak, thus sustaining much of the lateral heterogeneity in tracer concentrations arising from the two injection "sources" during transport downgradient. Figure 6 also shows that, over time, the position of the sub-plumes with respect to each other remained similar at the transect but that both sub-plumes moved laterally. The vertical black line in each frame is the x-coordinate of the middle of the injection zone, that is, between the two sets of wells used to create the sub-plumes. Frames (a) to (d) show that the path of the sub-plumes was nearly orthogonal to the well network during the first 128 d of the experiment (mid July through mid November, 2005); this is also evident in Figure 5a. However, in frames (e) to (g) of Figure 6 an eastward shift of approximately 3 m (to the right in the figure) occurred during the short rainy season (roughly Days 150 to 250); a similar temporary eastward shift was noted in a prior experiment at the site (Mackay et al. 2006). Frames (h) to (l) show that the position of the sub-plumes moved westward a total of about 6 m after Day 250, that is, to about 3 m west of the initial position in frames (a) to (d). The slight variations in flow direction suggested by the plume movement (~±5 degrees if flow direction is assumed linear from injection wells to EH transect) were apparently too small to be evident in the hydraulic head data.

Estimation of Groundwater Discharge

Specific discharge of groundwater is equal to the product of hydraulic conductivity and hydraulic gradient. The estimated average hydraulic conductivity of the S3 sand is 13.7 m/d, based on pumping tests and calibration of a preliminary numerical model using the water level and bromide data (Malcolm Pirnie 2009). The area within which we estimated hydraulic gradients (and subsequently bromide mass discharge) in this paper is indicated by the trapezoid in Figure 5a. For horizontal gradient estimation, we assumed that there was negligible vertical gradient within the S3 aquifer and utilized head data from wells in the EC, ED, EH, and/or EJ transects (Table 1). For 11 of the 13 head snapshots the data allowed reliable estimation of the hydraulic gradient within the trapezoidal area in Figure 5a by linear regression of the head data vs. distance along the direction of flow; there was no evidence of significant variation of gradient spatially within the trapezoidal area. Figure 7 plots these estimates with their 95% confidence intervals vs. time. Narrow confidence intervals resulted because we could identify and ignore outliers at a given transect resulting from occasional measurement errors since the majority of the head data were consistent at the transect. Assuming the hydraulic gradient was constant in space and time, that is, that the apparent variation in the figure was due to measurement error, the average gradient and 95% confidence interval was 0.0132 ± 0.0004.

Preliminary modeling suggested that the pumping would have affected the head at (and thus the hydraulic gradient in the vicinity of) the EJ transect, but would have had negligible effect at or upgradient of the EH transect.

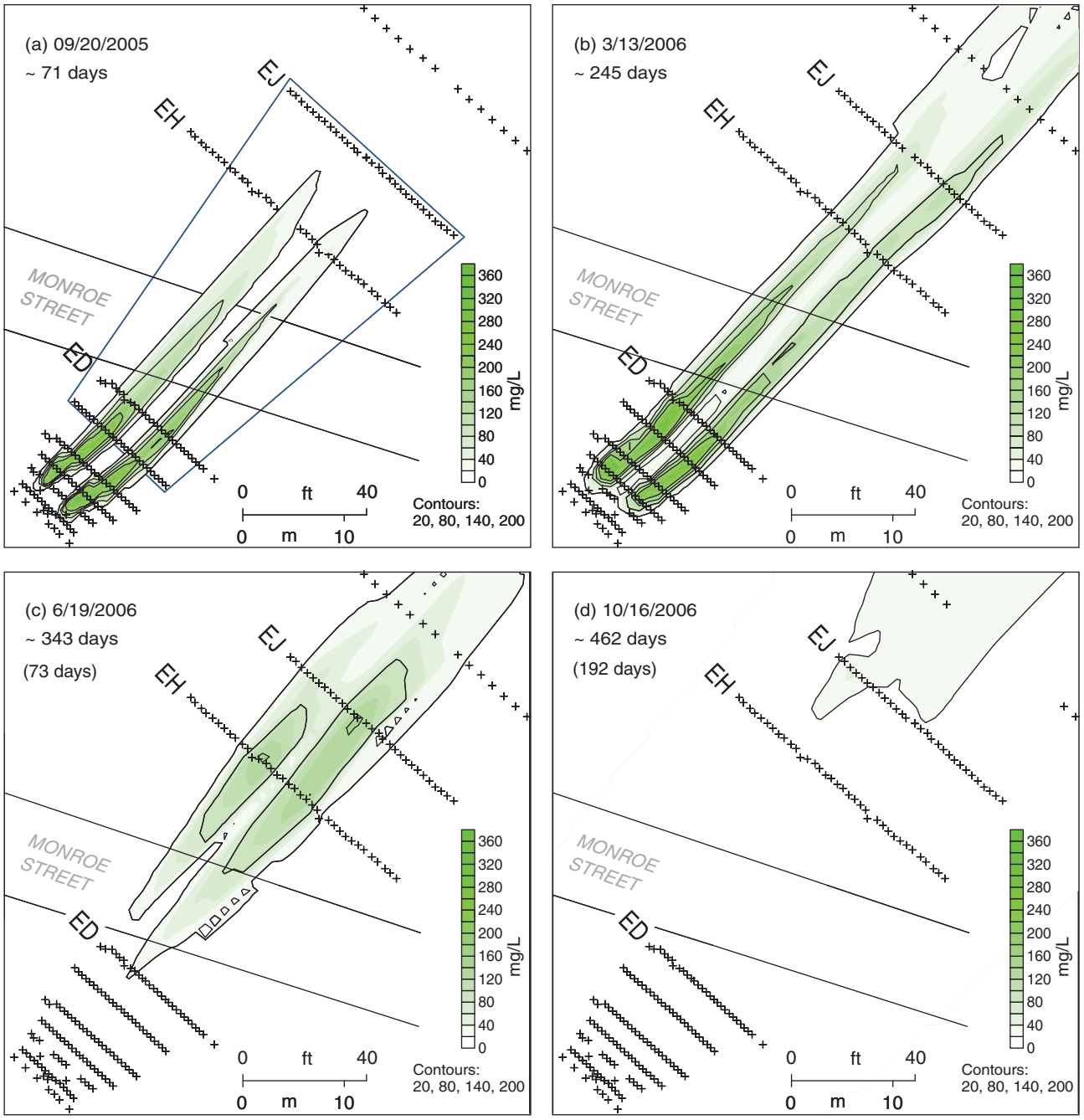

Figure 5. Contour plots of bromide plume. Frames (a) and (b) show growth of bromide sub-plumes during bromide injection; days after start of injection are listed below date. Frames (c) and (d) show bromide sub-plumes flushing from aquifer after cessation of bromide injection on Day 299; days after cessation are shown in parentheses. Marks (x) depict all wells sampled for each snapshot (wells not sampled are not depicted). The blue trapezoid in frame (a) encloses the wells used for estimation of hydraulic gradient and the transects used for estimation of bromide M_d (ED, EH, and EJ).

Figure 7 is consistent with the model expectations since the estimated hydraulic gradient was quite constant in space and time over the course of this experiment for the limited area of focus for this analysis, provided EJ data were not included in gradient estimation during the low-rate EJP pumping periods (Table 1). We expect that the gradient at the EJ transect would have been increased slightly during the EJP pumping periods, but do not have sufficient field data to make reliable estimates of the increase in gradient at EJ during those times.

Therefore, hereafter we assume that the gradient is constant in space and time in the experimental area. Given the assumed average hydraulic conductivity and assuming the effective porosity is 70% to 100% of the total porosity (0.34), the average linear groundwater velocity within the zone of interest during this test is estimated to be within the range 0.53 to 0.76 m/d, that is, similar to the range of estimates from prior years of research at the site (0.5 to 0.75 m/d) and preliminary numerical modeling (Malcolm Pirnie 2009). During this research there was no evidence

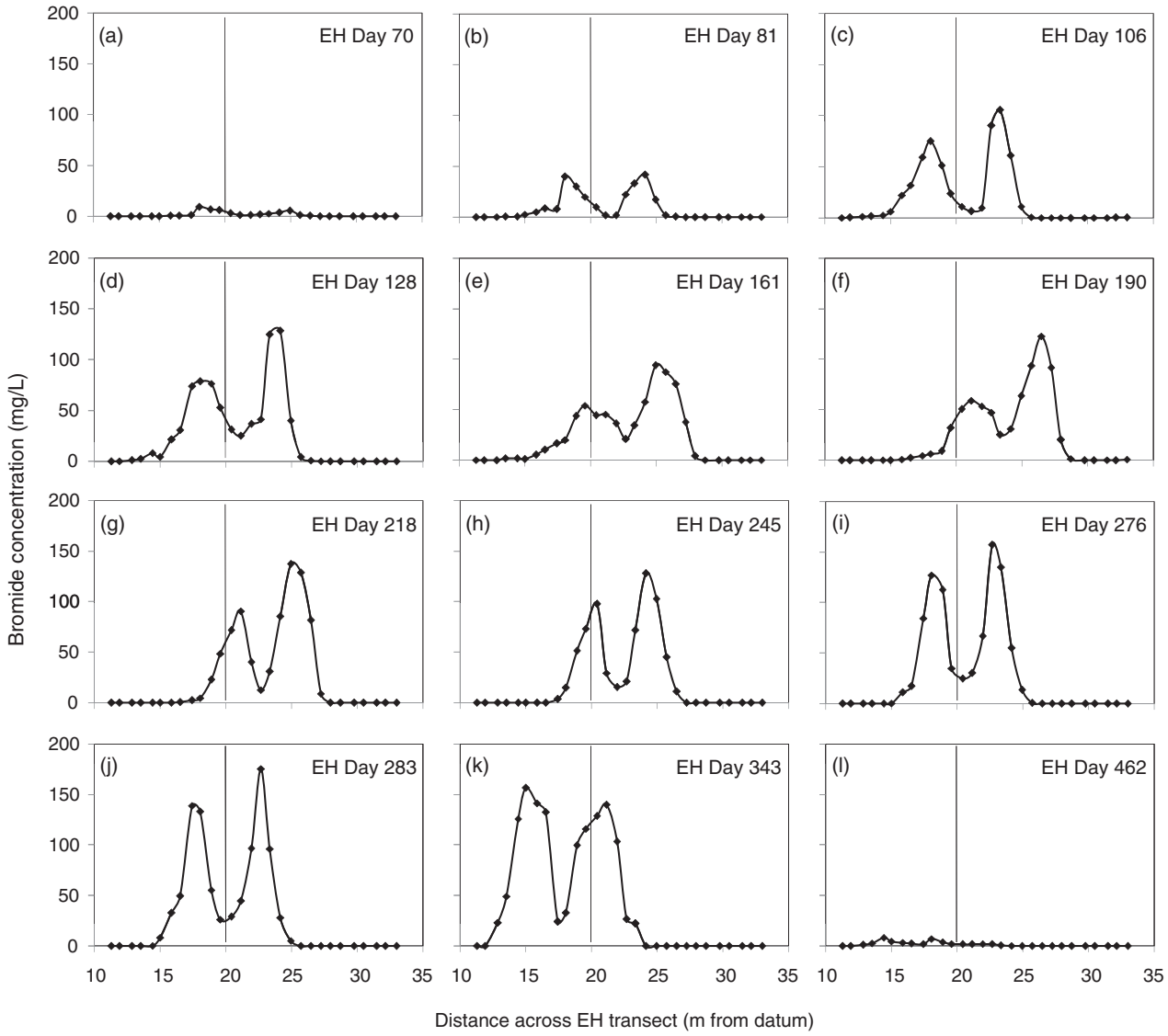

Figure 6. Bromide concentration across EH transect for 12 snapshots. Data are plotted vs. distance across the transect measured from an assumed datum (*y*-axis depicted in Figure 1). The black vertical black lines in the frames show the expected center of the sub-plumes for flow along the assumed mean flow direction.

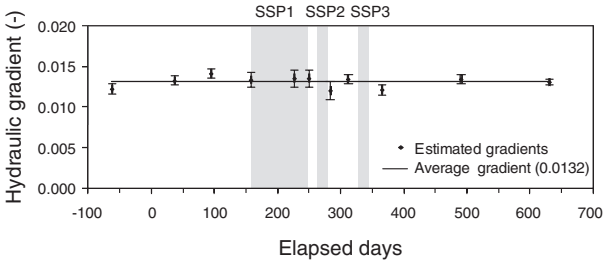

Figure 7. Estimated hydraulic gradient (and 95% confidence interval) for the area noted in Figure 5a from before the experiment began (Day 0) to after all EH monitoring was complete (Day 462). Gray shading indicates durations of the continuous pumping events in the EJP transect.

of significant seasonal variations in the magnitude of the hydraulic gradient, and thus groundwater velocity, within the trapezoid in Figure 5a.

Estimation of Bromide Mass Discharge (M_d)

Figure 8 presents estimated bromide M_d, calculated using Equation 1, for each snapshot of the ED, EH, and EJ transects. Estimates for the EJ transect are included in this and a subsequent plot despite the expectation that they are slightly inaccurate due the impact of periods of pumping at the EJP, as discussed earlier. Figure 8 shows migration of the injected bromide mass past each transect, with peaks and valleys which arise, in part, from variations in the bromide injection rate over time (changes in slope in Figure 4). Figure 8 also indicates tailing in the elution of bromide (particularly evident in the EJ plot), an expected impact of bromide diffusion into and subsequently out of the lower permeability strata above and below the thin S3 aquifer (Figure 2). Note that site-specific modeling using the approach of Rasa et al. (2011) confirms that known variations in injection rates result in breakthrough plots with temporal variations similar

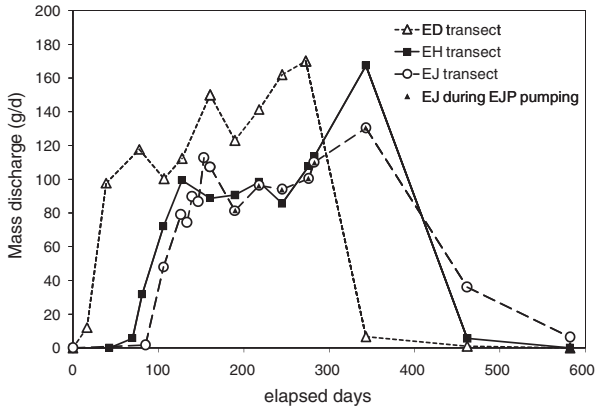

Figure 8. Bromide mass discharge estimated by the Theissen Polygon Method (TPM) over the duration of the experiment at transects ED, EH, and EJ using all wells in each transect. Monitoring captured the migration of the injected plume past each transect (breakthrough and elution). The solid triangles in some of the EJ data indicate times during which pumping was occurring in the EJP transect, discussed in text.

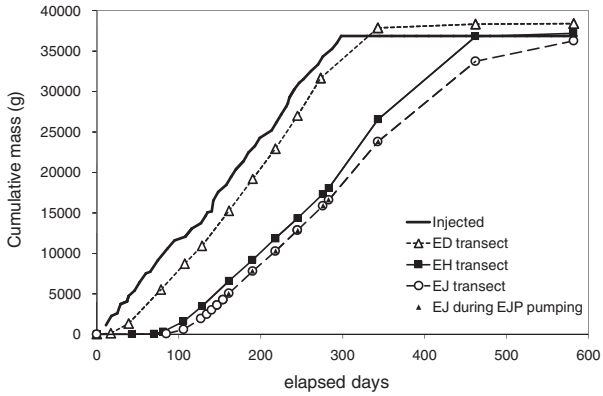

Figure 9. Estimated total cumulative mass discharged through transects ED, EH, and EJ compared to known cumulative mass of bromide injected. Estimates for each transect were generated by integration of area under plots in Figure 8. The solid triangles in some of the EJ data indicate times during which pumping was occurring in the EJP transect.

to those in Figure 8 and suggests that less than 5% of the injected bromide was temporarily immobilized within the silty units over- and under-lying the S3 aquifer upgradient of the EJ transect at any given time. Though additional modeling analyses of the dataset are forthcoming, it is not necessary to await those results to draw more insight directly from the monitoring data and TPM estimates.

Mass Balance and M_d Estimation Error

The total mass of bromide that migrated past the ED, EH, or EJ transects over time was estimated as the area under the plots in Figure 8, assuming linear interpolation between the points (Levenspiel 1979). Figure 9 shows that the estimated cumulative mass at the end of the sampling period varies only slightly (<6%) among the transects; all are within 4% of the total bromide mass injected. The good mass balance suggests that the TPM method for analyzing the detailed snapshot sampling data is quite accurate. Since the hydraulic gradient at the EJ transect during the periods of EJP pumping was likely slightly higher than assumed, some of the M_d and cumulative mass estimates in Figures 8 and 9 (denoted with the solid triangles) may be slightly underestimated. The apparent mass balance accuracy for the ED and EH transects may be to some degree an artifact of fortuitous assumptions made in the integration of the M_d history or in calculations of M_d at each time. However, since the total mass was apparently accurately estimated at all three transects, it appears that the M_d histories at each transect were well defined by the reasonably regular and frequent sampling.

Regarding the estimation of the M_d values, it is conceivable that errors in some assumptions counterbalanced errors in others. The most certain of the parameters in Equation 1 are the bromide concentrations, given the low estimated error (<1%). The hydraulic gradient is also very accurately known, with low potential error (95% CI is ~3% of the average estimated gradient). For our case with fully penetrating wells, the sampled Area A is defined by the TPM as the product of the aquifer thickness and the represented width, which is calculated from the distances between the screened sections of the wells. The uncertainty in the estimates between tops of wells is very low, perhaps 1 cm, that is, 1.3% of the average inter-well distance in the EH transect (0.77 m). The error in the estimated distances between well screens may be higher if the wells are not installed perfectly vertically, but the direct push method of well installation in this work likely resulted in relatively small deviations from vertical installation for these shallow wells. Thus in our case the most uncertain of the parameters used to estimate M_d for the ED and EH transects were the hydraulic conductivity (K) and the aquifer thickness. Errors in these parameters could easily balance out: for example, if the true K was 10% higher than we had estimated, the same M_d would be estimated if true thickness were 10% lower than we had estimated. Errors of this magnitude for estimates of K would not be surprising. We believe such an error is also possible for estimating thickness for our very thin aquifer (0.9 m) given the inevitable uncertainty in defining contacts between geologic strata where contacts are gradational, as in this case. If we assume the errors in the various parameters are independent and use standard methods for error propagation, the expected errors would be approximately 5% for each calculated M_d and approximately 2% for the cumulative total mass estimate for each transect, which agrees well with results in Figure 9.

It is possible that the reason for the differences between total masses detected at the ED and EH transects, although small, is that specific discharge and/or aquifer thickness varied somewhat throughout the experimental area. Examination of Figure 5 suggests that groundwater velocity (and thus also specific discharge) may vary slightly between the pathways followed by the east and west sub-plumes, so the assumption herein of spatial

Table 2
Subsets of EH Transect Sampling Data Used for Estimation of Bromide Mass Discharge

Average Well Spacing		Sample Density[1]			
(m)	(ft)	(points/m^2)	Number of Subsets	Number of Wells in Each Subset	Total Number of Subset M_d Estimates
0.77	2.54	1.4	1	29	12
1.55	5.10	0.70	2	15, 14	24
2.33	7.64	0.47	3	10, 10, 9	36
3.10	10.18	0.35	4	8, 7, 7, 7	48
3.87	12.70	0.28	5	6, 6, 6, 6, 5	60
4.63	15.20	0.24	6	5, 5, 5, 5, 5, 4	72
5.39	17.70	0.20	7	5, 4, 4, 4, 4, 4, 4	84

Notes: The full set of wells was taken as EH08 through EH36; we did not include EH01 to EH07 in calculations for and plots in Figures 10 to 12 since they were always outside the plume.
[1]Calculated from average well spacing, assuming 3 feet (~0.9 m) average aquifer thickness.

uniformity in specific discharge may be an oversimplification. However, it is a common practice to assume spatial uniformity in discharge, since available data cannot typically support more complex assumptions. Thus we make that assumption in calculations herein.

Potential M_d Error for Sparser Sampling Densities

In reality, plume cross sections often display considerable spatial variability in concentration in both the horizontal and vertical directions, and consequently several prior studies have concluded that the error in M_d estimation is generally lower for high sampling densities (sampling points per m^2). In this work, we have the unusual advantage of knowing that the M_d estimates using the detailed transects are reasonably accurate. We thus have the opportunity to provide additional insight into the impact of sampling density and location. In the rest of this paper, we focus attention on the EH transect, though similar conclusions arise from examining data from the ED transect. Since we used fully penetrating wells in our study, sampling density is directly related to well spacing. Therefore, evaluation of the impact of sampling density was accomplished by using various subsets of the EH transect data with sparser well spacing (Table 2).

For this analysis, we included 29 of the 36 wells in the EH transect (EH08 to EH36), that is, the portion of the transect within which the plume remained over the experiment. Hypothetical subsets with reasonably regular spacing were selected by assuming only every other well had existed, then assuming only every third well, and so on. The full set and hypothesized subsets thus had well spacings in the range 0.77 to 5.39 m and sampling densities in the range 1.4 to 0.20 points/m^2. Note that for well spacings of 1.55 m and higher there were different subsets of wells to be considered: for 1.55 m spacing, a subset with 15 and a subset with 14 wells; for 2.33 m spacing, one subset with 9 wells and two subsets with 10 wells, and so on.

Using the TPM, the bromide M_d was calculated for the 12 EH snapshots depicted in Figure 6 and for all of the various subsets of EH data listed in Table 2. This resulted in 336 estimates of bromide M_d at the EH transect, ranging from times when bromide mass discharge at the monitored transect was low to times when it was high. This approach allowed examination of the effect of sampling a laterally variable bromide distribution with a fixed well spacing (and thus fixed sampling density), yet with different locations with respect to the sub-plumes.

The effect on M_d estimation of varying the well spacing is summarized in Figure 10. We adopt the approach of Beland-Pelletier et al. (2011), by taking the "best" estimate of M_d calculated using all 29 EH wells as the "true" value of M_d at the sampling time. The RPD between selected M_d estimates for the hypothesized sparse transects ($M_{d,hyp}$) and the "true" M_d is defined by the following expression:

$$\mathrm{RPD} = 100\frac{(M_{d,hyp} - M_d)}{M_d}$$

RPD is plotted for all EH snapshots in Figure 10 vs. (a) average hypothesized well spacing, (b) sample density for the hypothesized transects, and (c) fraction of plume area sampled by the hypothesized transects.

Figure 10a suggests that for assumed well spacing of 3.1 m or less, there is generally less than a 30% error associated with the individual bromide M_d estimates for hypothesized subsets of the wells, whereas for assumed well spacing greater than 3.1 m the potential error increases dramatically. The potential error increases when well spacing is on the order of or wider than the sub-plumes (3 to 5 m, as indicated in the figure).

Figure 11 illustrates why different locations for a hypothesized sampling transect with a given well spacing yielded varying estimates of mass discharge. The frames present plots of bromide concentration vs. distance across the EH transect for one snapshot (283 d) for which the TPM estimated M_d using all 29 wells was 113 g/d. The frames illustrate the assumptions made by the TPM for three possible lateral locations of hypothesized sparse transects for three of the average well spacings

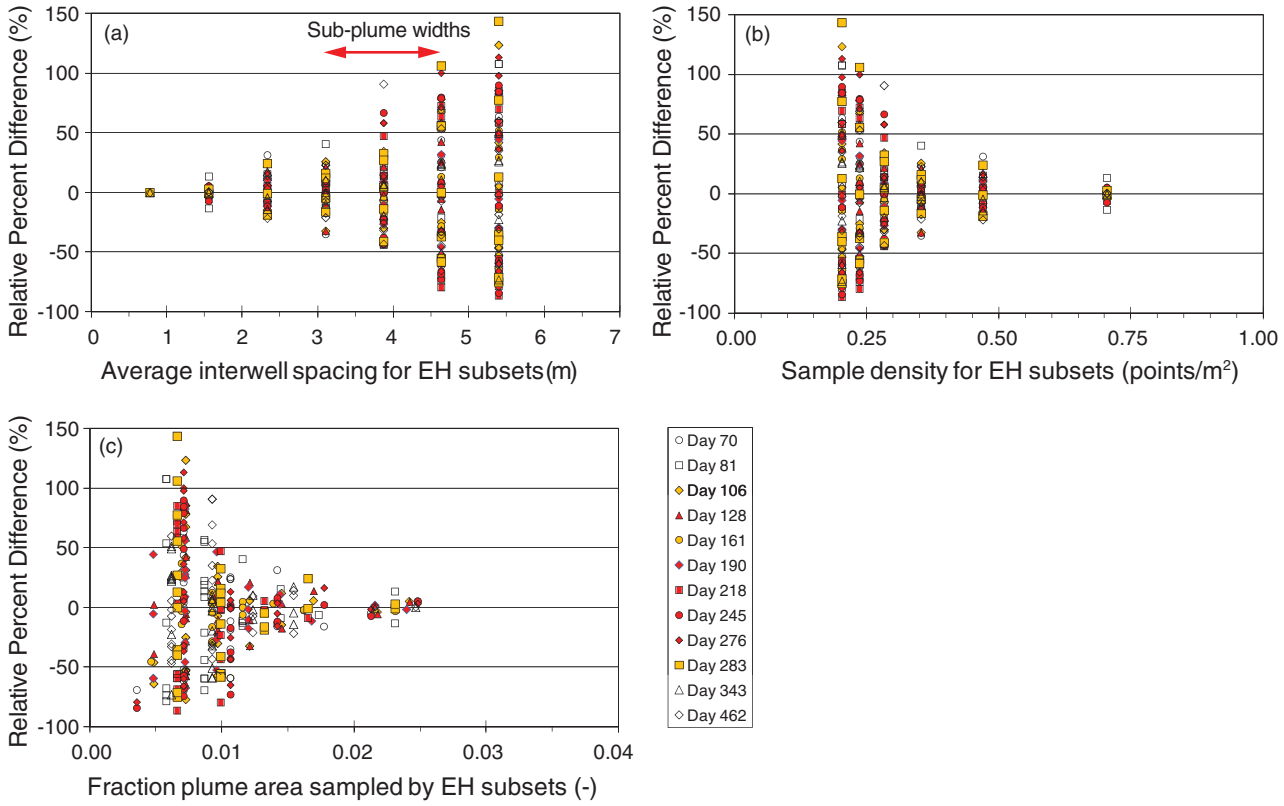

Figure 10. Estimated mass discharge (M_d) at the EH transect for subsets of EH wells (Table 2), plotted as relative percent difference (RPD) from the M_d estimated using all wells vs.: (a) well spacing, (b) sample density (ρ_s, points/m^2), and (c) the fraction of plume area sampled (f_s, unitless).

(2.33, 3.37, and 5.39 m). Frames (a) to (c) present the subsets that result in the M_d estimate with the highest positive RPD for that well spacing. Frames (d) to (f) and (g) to (i) present the subsets that lead to the M_d estimates with RPD closest to zero or RPD most negative, respectively. In each frame, the red filled circles mark the bromide results for the wells in each hypothesized subset and the green shading indicates the concentration distribution assumed by the TPM for that particular subset. In each plot, the black symbols and connecting line depict results for all 29 wells. Clearly, the hypothesized subsets depicted in frames (a) to (c) and (g) to (i) result in high and low RPD, respectively, because the area of the green shaded rectangles (which is proportional to the mass discharge when groundwater discharge is assumed constant) is so different from the area under the true concentration distribution (black lines). In frames (d) to (f) the area of the green shaded rectangles is similar to that under the true concentration distribution, thus resulting in low absolute values of RPD. But these frames illustrate that it is possible for TPM analysis of a sparse dataset to yield a mass discharge estimate close to the true value, even though poorly defining the actual concentration distribution. Overall, Figure 11 illustrates, as stated by Beland-Pelletier et al. (2011), that "uncertainty in mass discharge is dependent not only on the monitoring fence density and aquifer heterogeneity, but also on the chemical distribution at the fence." Figure 11 also implies that, for a plume in a uniform flow field, an M_d estimate with RPD near zero is gained by having monitoring data whose average value is near the true average concentration and whose locations yield an assumed total plume width close to the true plume width. As illustrated in frame (f), for a sparse transect in such a setting it is not necessary to monitor the highest concentration portion of each of the sub-plumes. In practice, of course, it is not possible to know what portion of the plume concentration distribution has been captured by a sparse transect unless: (1) detailed characterization has been conducted, ideally before transect installation, as suggested by others (Cai et al. 2011; Li and Abriola 2009), and (2) it is known or reasonably assumed that the plume location does not shift laterally at the transect over time.

On the other hand, if the plume does move laterally over time, as in this case and perhaps many others, there could be significant variations in estimated M_d over time due to flow direction changes, even if true M_d and groundwater velocity remained constant, since different portions of the plume would be sampled by a fixed transect as the plume shifted. The magnitude of this potential error increases as the spacing between sampling points increases. Figure 12 illustrates this by plotting RPD for all of the hypothesized EH subsets with well spacing from 2.33 to 5.39 m as a function of position of the hypothesized subset along the transect, where position is defined as lateral shift from the location of the subset

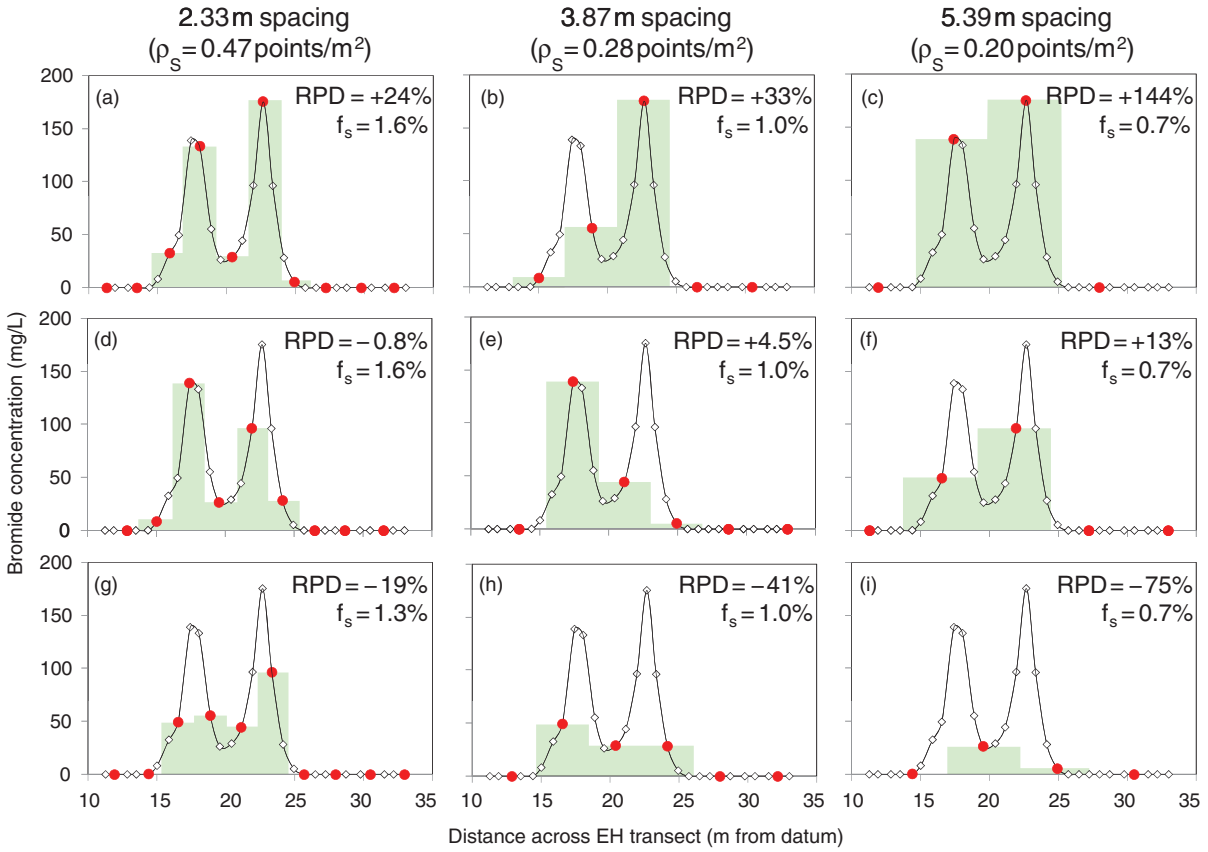

Figure 11. Measured concentration distribution (black symbols and connecting line) at the EH transect on Day 283 and that assumed by the Theissen Polygon Method (TPM) for three assumed average well spacings, with sample density (ρ_s) in parentheses. The red dots indicate the data used for the hypothesized subsets; the green rectangles indicate the concentration distribution assumed by the TPM. Frames (a) to (c) illustrate the TPM estimate for the hypothesized cases with highest RPD for the assumed well spacing. Frames (d) to (f) and (g) to (i) illustrate the cases with TPM closest to the "true" value and lowest compared to "true" value, respectively, for the assumed well spacing. Noted in each frame are the RPD and the fraction of plume area sampled f_s (in percent).

with lowest absolute value of RPD (i.e. the most accurate subset). Figure 12 shows that the RPD varies with shift in assumed location of the transect, with a greater range in RPD for larger hypothesized well spacings, as expected. Note that only a 1-meter shift in transect position results in a significant change in RPD for the sparser transects. Thus even small shifts in flow direction may potentially have significant impacts on mass discharge estimation using sparse transects to monitor laterally heterogeneous plumes, at least for nonsorbing or weakly sorbing contaminants. The impact of slight changes in flow direction may be less significant for contaminants that are more strongly sorbing since the lateral shift in plume location could be lessened by retardation of the sorbing solute. Also, denser networks of sampling points are much less vulnerable to the above-described errors caused by temporal shifts in the position of the plume in the aquifer, as illustrated in Figure 12. Finally, this issue would be less significant if the groundwater flow field was not uniform but constrained to high permeability flowpaths.

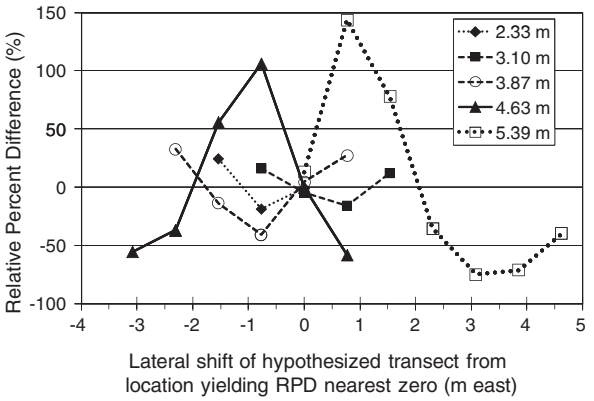

Figure 12. Plot of relative percent difference (RPD) between estimated M_d from hypothesized sparse EH transects to "true" M_d estimated using all 29 wells in EH transect (0.77 m spacing). Position is defined as meters eastward shift in location from the sparse transect yielding the lowest absolute value of RPD for each assumed well spacing.

Figure 10b presents RPD vs. sampling density (points/m^2), indicating that potential error increases as sampling density decreases. In this work, using fully penetrating wells to monitor a plume comprised of two lobes, each on the order of 4 m wide, a significant increase in potential error is noted when sampling density

falls below 0.4 points/m^2. This is consistent with results of prior studies. Beland-Pelletier et al. (2011) evaluated multilevel monitoring of a plume with two lobes, each approximately 2 m wide and 2 m high, noting that potential error increased significantly for sampling density less than 0.6 points/m^2. Cai et al. (2011) evaluated application of the TPM to multilevel sampling of a plume without multiple lobes, but with sharp concentration gradients, and found that predicted uncertainty of M_d increased substantially for sample density at or below 1 point/m^2. While the general agreement among these estimates is of interest, the relationship of potential error to sampling density must inevitably depend on the spatial distribution of the target solutes at the monitored transect, as discussed above, as well as the characteristics of the flow field (e.g., variation of specific discharge across the transect).

Li et al. (2007) suggested that the sum of the areas actually sampled by the wells (i.e., considering the volume of the aquifer from which the groundwater sample arises) could be a useful predictor of potential uncertainty in M_d estimates from transect sampling. Using synthetic data sets (77.3 m^2 cross-sectional area) monitored with four 6-point multilevel wells, and making an assumption regarding lateral sampling width of the multilevel well points (0.3 m), they concluded that accurate assessments of uncertainty for highly heterogeneous plumes (i.e., multi-lobed, with hot spots and large areas of near zero concentration) require a sampling density of at least 6 to 7% of the cross-sectional area of the transect for a regular monitoring grid. In their case, the hypothesized grid did not extend far beyond the plume itself. In Figure 10c we followed their approach, but determined the sampling density relative to the known width of the plume at each sampling time, to avoid bias arising solely from transect widths much greater than plume widths, which may occur for a variety of reasons in practice. To estimate the fraction of the plume that was sampled, we assumed, as a first approximation, that the hydraulic conductivity of the S3 aquifer was uniform vertically and that the pumping during our sampling process yielded a steady state capture zone; the latter is a reasonable assumption for reasons discussed elsewhere (Malcolm Pirnie 2009). Using a 2D numerical model accounting for well and aquifer characteristics, we estimated the width sampled by each well during the brief sampling time as 3.5 cm. Therefore, since the average well spacing of our EH transect was 0.77 m, our snapshots using all EH wells sampled approximately 4.5% of the cross sectional area of the EH transect. The apparent accuracy of the M_d estimates using all EH wells is consistent with the conclusion of Li et al. (2007) that sampling densities greater than 4% to 5% would yield M_d errors under 10%. Of more practical relevance is the fraction of the cross-sectional area of the plume that would be sampled by sparser (more typical) transects. Fraction of plume area sampled (f_s) for each of the hypothetical sparse well subsets, and for all snapshots, is presented in Figure 10c, which illustrates that potential error increases substantially for fractions of plume area sampled lower than 0.012.

Conclusions and Implications

Mass discharge (M_d) measurements made via application of the TPM to snapshot sampling data for a thin, laterally heterogeneous plume in a relatively uniform flow field were quite accurate in this study for transects of closely spaced, fully penetrating wells. Errors in M_d estimates by the TPM for uniform aquifers should be relatively low (±30%) if the well spacing is regular and less than the width of the high concentration sub-plumes (also known as "plume cores"). However, for laterally heterogeneous plumes sampled with sparse transects, as is more typically the case in practice, the accuracy of the snapshot method may strongly depend on the location of wells relative to the sub-plumes, especially if sub-plume locations change significantly over time due to shifts in groundwater flow direction. Changes in M_d which arise solely from lateral plume shifts might be misinterpreted as resulting from other processes, such as in situ biodegradation, confounding decisions about site management. Similar conclusions would be expected for thicker plumes with significant lateral and vertical concentrations variations across transects, as noted by others (Beland-Pelletier et al. 2011; Cai et al. 2011).

Assuming uniform aquifer properties and hydraulic gradient, as would typically be done in practice, may introduce positive or negative biases which would be difficult to quantify. However, for applications in which the primary goal is comparing M_d over time at a given transect, fractional changes in M_d can still be determined accurately if hydraulic gradient and groundwater flow direction do not vary significantly and if the transect well spacing is dense enough to characterize the average concentration and width of the plume.

Finally, it has been suggested that the accuracy of the snapshot method can be improved by pre-characterizing the geology and solute distribution along the measurement transect(s) prior to creating permanent monitoring transects (EPA 2005; Li et al. 2007; Cai et al. 2011). With such information, denser networks of monitoring devices could be installed in and near the high mass flux zones. However, at sites where the positions of high-concentration sub-plumes shift over time, more laterally extensive networks of sampling points still may be necessary to track changes in the location of the plume cores and obtain accurate estimates of M_d using the TPM. However, if flow direction shifts are reasonably predictable, sampling conducted when flow is known or likely to be in a preferred direction can potentially allow more useful comparisons of M_d over multiyear time frames, such as required for performance evaluation of natural attenuation or engineered remediation systems.

Acknowledgments

Primary funding for the field experimental work was provided by a subcontract to UC Davis by Malcolm Pirnie, Inc., the primary contractor to the Environmental Security Technology Certification Program (ESTCP) for project ER-0318. Seed funding was provided by

the American Petroleum Institute (API). In addition, Geomatrix Consultants (now AMEC Geomatrix) provided monetary support and field assistance. Since 2006, additional data analysis was funded by the American Petroleum Institute (contract 2010-104864), the University Consortium for Field Focused Groundwater Contamination Research, and Award Number P42ES004699 from the National Institute Of Environmental Health Sciences. The content is solely the responsibility of the authors and does not necessarily represent the official views of the National Institute of Environmental Health Sciences or the National Institutes of Health. Valuable assistance was provided by Madalena Velasco, Larry Justice, Max Justice, Veronica Morales, Anthony Parker and Chloe Lucado (UC Davis), and Michael Kavanaugh, Rula Deeb and Elisabeth Hawley (Malcolm Pirnie, Inc.). The authors thank Vandenberg Air Force Base staff, especially Mike McElligott, Pablo Martinez, Andy Edwards, Ron MacLelland, Craig Nathe and Kathy Gerber, and staff of the Regional Water Quality Control Board, San Luis Obispo, CA especially Carol Kolb, Bill Meece, Kristina Seley and Linda Stone. We thank three anonymous reviewers for helpful comments.

References

Beland-Pelletier, C., M. Fraser, J. Barker, and T. Ptak. 2011. Estimating contaminant mass discharge: A field comparison of the multilevel point measurement and the integral pumping investigation approaches and their uncertainties. *Journal of Contaminant Hydrology* 122, no. 1–4: 63–75.

Cai, Z., R.D. Wilson, M.A. Cardiff, and P.K. Kitanidis. 2011. Increasing confidence in mass discharge estimates using geostatistical methods. *Ground Water* 49, no. 2: 197–208.

Chapman, S.W., B.T. Byerley, D.J.A. Smyth, and D.M. Mackay. 1997. A pilot test of passive oxygen release for enhancement of in situ bioremediation of BTEX-contaminated ground water. *Ground Water Monitoring & Remediation* 17, no. 2: 93–105.

Clements, L., T. Palaia, and J. Davis. 2008. Characterisation of sites impacted by petroleum hydrocarbons. National Guideline Document. CRC for contamination Assessment and Remediation of the Environment (Australia). Report No. 11. 122 p.

Dietze, M., and P. Dietrich. 2011. A field comparison of BTEX mass flow rates based on integral pumping tests and point scale measurements. *Journal of Contaminant Hydrology* 122, no. 1–4: 1–15.

Einarson, M.D., and D.M. Mackay. 2001. Predicting impacts of groundwater contamination. *Environmental Science & Technology* 35, no. 3: 66A–73A.

EPA. 2005. Groundwater sampling and monitoring with direct push technologies. OSWER. United States Environmental Protection Agency 540/R-04/005. 78 p.

Feenstra, S., J.A. Cherry, and B.L. Parker. 1996. Conceptual models for the behavior of dense non-aqueous phase liquids (DNAPLs) in the subsurface. In *Dense Chlorinated Solvents and Other DNAPLs in Groundwater: History, Behavior, and Remediation*, ed. Pankow, J.F., and J.A. Cherry, 53–88. Portland, Oregon: Waterloo Press.

Guilbeault, M.A., B.L. Parker, and J.A. Cherry. 2005. Mass and flux distributions from DNAPL zones in sandy aquifers. *Ground Water* 43, no. 1: 70–86.

ITRC. 2010. Use and measurement of mass flux and mass discharge. Integrated DNAPL Site Strategy Team, The Interstate Technology & Regulatory Council, 154 p.

Kübert, M., and M. Finkel. 2006. Contaminant mass discharge estimation in groundwater based on multi-level point measurements: A numerical evaluation of expected errors. *Journal of Contaminant Hydrology* 84, no. 1–2: 55–80.

Levenspiel, O. 1979. *The Chemical Reactor Omnibook.* Corvallis, Oregon: Oregon State University Bookstore. ISBN 0-88246-067-6.

Li, K.B., and L.M. Abriola. 2009. A multistage multicriteria spatial sampling strategy for estimating contaminant mass discharge and its uncertainty. *Water Resources Research* 45: W06407. DOI: 10.1029/2008WR007362.

Li, K.B., P. Goovaerts, and L.M. Abriola. 2007. A geostatistical approach for quantification of contaminant mass discharge uncertainty using multilevel sampler measurements. *Water Resources Research* 43: W06436. DOI: 10.1029/2006WR005427.

Mackay, D.M., N.R. De Sieyes, M.D. Einarson, K.P. Feris, A.A. Pappas, I.A. Wood, L. Jacobson, L.G. Justice, M.N. Noske, K.M. Scow, and J.T. Wilson. 2006. Impact of ethanol on the natural attenuation of benzene, toluene, and o-xylene in a normally sulfate-reducing aquifer. *Environmental Science & Technology* 40, no. 19: 6123–6130.

Malcolm Pirnie. 2009. Estimation of mass discharge of groundwater contaminants: A controlled field comparison of four methods at Vandenberg Air Force Base, CA. ESTCP Project Number: ER-0318, Project Report v.2, June 2009, 102 p.

Newell, C.J., S.K. Farhat, D.T. Adamson, and B.B. Looney. 2011. Contaminant plume classification system based on mass discharge. *Ground Water* 49, no. 6: 914–919. DOI: 10.1111/j.1745-6584.2010.00793.x.

Newell, C.J., J.A. Conner, and D.L. Rowen. 2003. *Groundwater Remediation Strategies Tool.* American Petroleum Institute. Publication Number 4730. 80 p.

Pope, D.F., S. Acree, H. Levine, S. Mangion, J. van Ee, K. Hurt, and B. Wilson. 2004. Performance monitoring of MNA remedies for VOCs in ground water, National Risk Management Research Laboratory (NRMRL), Ada, Oklahoma, Publication EPA/600/R-04/027, 92 p.

Rao, P.S.C., J.W. Jawitz, C.G. Enfield, R.W. Falta, M.D. Annable, and A.L. Wood. 2002. Technology integration for contaminated site remediation: clean-up goals and performance criteria. In *Groundwater Quality: Natural and Enhanced Restoration of Groundwater Pollution (Proceedings of the Groundwater Quality 2001 Conference held at Sheffield, UK,* June 2001), Wallingford, Royaume-Uni, International Association of Hydrological Sciences.

Rasa, E., S. Chapman, B. Bekins, G. Fogg, K. Scow, and D. Mackay. 2011. Role of back diffusion and biogeochemical reactions in sustaining an MTBE/TBA plume in alluvial media. *Journal of Contaminant Hydrology* 126: 235–247.